

Photoactivated Mixed In-Plane and Edge-Enriched p-Type MoS₂ Flake-Based NO₂ Sensor Working at Room Temperature

Abhay. V. Agrawal,[†] Rahul Kumar,[‡] Swaminathan Venkatesan,[§] Alex Zakhidov,[§] Guang Yang,^{||} Jiming Bao,^{||} Mahesh Kumar,[‡] and Mukesh Kumar^{*,†}

[†]Functional and Renewable Energy Materials Laboratory, Indian Institute of Technology Ropar, Punjab-140001, India

[‡]Department of Electrical Engineering, Indian Institute of Technology Jodhpur, Jodhpur-342011, India

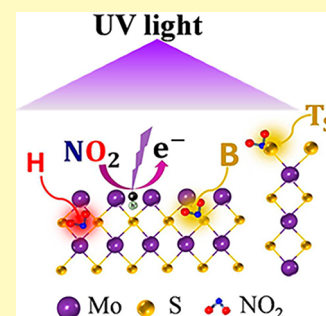
[§]Department of Physics, Texas State University, San Marcos, Texas 78666, United States

^{||}Department of Electrical Computer Engineering, University of Houston, Houston, Texas 77204, United States

Supporting Information

ABSTRACT: Toxic gases are produced during the burning of fossil fuels. Room temperature (RT) fast detection of toxic gases is still challenging. Recently, MoS₂ transition metal dichalcogenides have sparked great attention in the research community due to their performance in gas sensing applications. However, MoS₂ based gas sensors still suffer from long response and recovery times, especially at RT. Considering this challenge, here, we report photoactivated highly reversible and fast detection of NO₂ sensors at room temperature (RT) by using mixed in-plane and edge-enriched p-MoS₂ flakes (mixed MoS₂). The sensor showed fast response with good sensitivity of ~10.36% for 10 ppm of NO₂ at RT without complete recovery. However, complete recovery was obtained with better sensor performance under UV light illumination at RT. The UV assisted NO₂ sensing showed improved performance in terms of fast response and recovery kinetics with enhanced sensitivity to 10 ppm NO₂ concentration. The sensor performance is also investigated under thermal energy, and a better sensor performance with reduced sensitivity and high selectivity toward NO₂ was observed. A detailed gas sensing mechanism based on the density functional theory (DFT) calculations for favorable NO₂ adsorption sites on in-plane and edge-enriched MoS₂ flakes is proposed. This study revealed the role of favorable adsorption sites in MoS₂ flakes for the enhanced interaction of target gases and developed a highly sensitive, reversible, and fast gas sensor for next-generation toxic gases at room temperature.

KEYWORDS: p-type MoS₂ flakes, NO₂ sensor, edge-enriched MoS₂, CVD, photoactivated sensor, S vacancy



Environmental pollution is one of the biggest problems at the present time.¹ Certain air pollutant toxic gases like NO₂, NO, and CO₂ are the most common gases produced in the environment from vehicles, energy sources, and power plants that use fossil fuels.² NO₂ is one of the hazardous gas produced during the burning of the fossil fuels. When NO₂ reacts with moisture, it forms acid rain which is very harmful to ecosystems.^{3,4} Furthermore, NO₂ is a decomposition product of many explosives.³ Therefore, the development of a highly sensitive and reversible NO₂ gas sensor at RT is a critical requirement for civil and environmental applications. Commercially developed NO₂ gas sensors are based on metal oxide semiconductors like WO₃, ZnO, In₂O₃, ZnO, V₂O₅, and MoO₃ due to their high sensitivity.^{5–7} However, the large response and recovery time, high working temperature requirement, and poor selectivity of metal oxide semiconductors have restricted their use for fast detection of the NO₂ gas. Recently, MoS₂ semiconductors have emerged as potential candidates in electrical and optical applications due to the thickness dependent tunable band gap, high surface to volume ratio, and high on/off switching ratio.^{8,9} The direct band gap and fast charge transport in single-layer MoS₂ provides applications for next generation nanoelectronic devices, energy storage, and

light-emitting diodes.^{10,11} Furthermore, MoS₂ is being explored for potential application in the area of hazardous gas sensing due to its high surface area for target gas interaction, direct band gap, and fast charge transport.^{9,11} Recently, the MoS₂ gas sensor has been reported for H₂, NH₃, H₂S, NO₂, and CO₂.^{11–13} However, MoS₂ based NO₂ gas sensors still suffer from the long response and recovery time, especially at RT.^{14,15} These problems were addressed by forming a composite structure of MoS₂ with Pt, rGO, and MoS₂/graphene hybrid aerogel and others to increase the interaction of the target gas with the sensing material.^{15–17} However, these strategies lead to increased complexity and cost in device fabrication. Furthermore, operating the device at elevated temperature was observed to decrease the response and recovery time, but at the cost of poor sensitivity.¹⁸ Recently, the presence of active sites, S vacancies, and defects was observed to enhance the catalytical properties of MoS₂ for hydrogen evolution reactions and electrochemical applications.^{10,19,20} Moreover, active sites, S vacancies, and defects play an important role in gas sensing

Received: February 16, 2018

Accepted: April 17, 2018

Published: April 17, 2018

applications.^{11,21} It has been reported that gas molecule interaction can be enhanced preferentially by the presence of the S vacancies and defects in MoS₂ flakes which increases the sensitivity, response time, and recovery of the sensor.^{11,22} So, controlling the active sites and defects can be helpful to develop highly sensitive, fast recovering, and reversible NO₂ gas sensor. Until now, there have been no experimental reports on the study of favorable adsorption sites for NO₂ gas molecules on the MoS₂ flakes. Thus, developing better-adsorbing favorable sites in MoS₂ flakes for NO₂ gas may help in developing highly sensitive, selective, and reversible NO₂ gas sensors even at room temperature.

Here, we are reporting NO₂ gas sensing on mixed in-plane and edge-enriched MoS₂ (mixed MoS₂) flakes. The sensor performance tested at moderate temperature shows a fast response and recovery with reduced sensitivity, while UV assisted NO₂ gas sensing shows high sensitivity, fast response, and reversibility behavior at RT for 10 ppm NO₂ gas. Finally, a detailed sensing mechanism is proposed based on the favorable adsorption sites available at the edges and in-plane sites of MoS₂ flakes and their interaction energy using density functional theory (DFT). We believe that the present work will give direction to the research community for the development of highly sensitive and selective gas sensors for the target gas depending on their favorable adsorption sites on the MoS₂ flakes.

EXPERIMENTAL WORK

Synthesis of Mixed MoS₂ Flakes. Mixed MoS₂ flakes were synthesized on a SiO₂/Si substrate by the modified atmospheric pressure chemical vapor deposition (APCVD) technique (details are discussed elsewhere¹¹). Before mixed MoS₂ growth, the SiO₂/Si substrate was sonicated in acetone for 20 min. High-purity MoO₃ powder (99.97%, Sigma-Aldrich) and sulfur powder (99.98%, Sigma-Aldrich) were used as a source for the growth of the mixed MoS₂ flakes. A small tube with one end closed loaded with powders and substrate was placed inside a bigger quartz tube in such a way that the closed end faced the gas inlet (see Supporting Information Figure S1). Ar gas flow was maintained at 150 sccm throughout the deposition. The closed end of the small tube was in zone 1 (MoO₃) and the open end was in zone 2. The growth temperature for zone 1 and zone 2 was fixed at 800 and 350 °C, respectively (see Figure S1). The growth time was 30 min followed by cooling to RT at the same Ar flow.

Characterizations and Device Fabrication of Mixed MoS₂ Flakes. HORIBA IHR 320 spectrometer was used to study the Raman and photoluminescence of MoS₂ flakes. A 532 nm laser at 500 μW power was used as the excitation source with a laser spot size of 0.5 μm. FEI Helios Nano Lab 400 with a probe current of 0.34 nA and an accelerating voltage of 10 kV was used to analyze the surface morphology of the MoS₂ flakes. Phase composition and crystal structure were analyzed by using a Rigaku Smart Lab diffractometer. For sensor fabrication, circular metal contacts of Au/Cr with the thickness of 250/3–5 nm having 100 μm diameter and separated by 100 μm were deposited by thermal evaporation.

Gas Sensing Measurements of Mixed MoS₂ Flakes. The sensing performance was evaluated at RT, RT under UV light (UV-LED lamp having a wavelength of 365 nm), and at moderate temperature of 125 °C for different concentrations of NO₂. The sensor selectivity is investigated with H₂, H₂S, CO₂, and NH₃ gases. Sensor performance was evaluated using a computer-controlled Keithley 4200 system. All gas sensing experiments were performed at constant relative humidity of ~32.06% in the same experimental setup for all temperatures (RT, RT+UV, and 125 °C). The humidity was measured by humidity sensor (SHT31-APR, Sensirion AG, Switzerland). A LED source (365 nm, 3 W, Taiwan light macro chip) with a light intensity of 1 mW/cm² was calibrated before the experiment using a calibrated photodiode (model FDS100–CAL) from Thorlab.

RESULTS AND DISCUSSION

Field emission scanning electron microscopy (FE-SEM) technique is carried out for the morphology analysis of the mixed MoS₂ flakes and the results are shown in the Figure 1a,b.

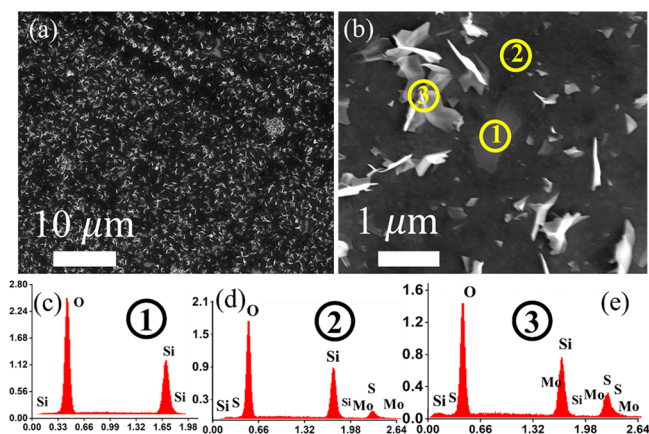


Figure 1. (a,b) FE-SEM image of as-synthesized mixed MoS₂ flakes. Spot EDS at three different locations: (c) EDS corresponding to the bare SiO₂/Si substrate at location 1; (d) EDS at location 2 on in-plane MoS₂ flakes; (e) EDS at the location 3 on edge-enriched MoS₂ flakes.

The blackish region is the in-plane MoS₂ flakes and the white region is the edge-enriched MoS₂ flakes. The edge-enriched MoS₂ flakes may appear white due to their height from the substrate surface. Figure 1b shows the high-resolution FE-SEM image of the same sample. Figure 1b indicates the mixed growth of the in-plane (blackish region, spot 2) as well as edge-enriched MoS₂ flakes (white region, spot 3) on the SiO₂/Si substrate.

The EDS measurements performed for the three locations of the mixed MoS₂ flakes. Location 1 corresponds to the bare SiO₂/Si substrate while locations 2 and 3 correspond to MoS₂ flakes. The EDS correspond to the bare substrate shown in the Figure 1c. Locations 2 and 3 shown in Figure 1d,e have S and Mo peaks with the O and Si. The O and Si peaks are coming from the SiO₂/Si substrate. The FE-SEM and spot EDS measurement confirm that the grown sample is mixed MoS₂ flakes.

To further confirm the MoS₂ flakes, Raman and PL spectroscopy have been performed on the mixed MoS₂ flakes. Figure 2a shows Raman spectra of the mixed MoS₂ flakes. Raman spectra of MoS₂ flakes consist of two lattice vibration peaks named E_{2g}¹ and A_{1g}. The E_{2g}¹ mode occurs due to the in-plane vibration of the S and Mo atoms while the A_{1g} mode is due to the out-of-plane vibration of the S atoms.^{23,24} The average peak position difference ($\Delta \approx A_{1g} - E_{2g}^1$) and peak intensity ratio (E_{2g}¹/A_{1g}) for these peaks are 24.86 cm⁻¹ and 0.42, respectively. PL spectra obtained from the mixed MoS₂ flakes show two prominent well-reported peaks A and B (Figure 2b).²⁵ The PL spectra were recorded at the same spots where Raman spectra were collected. The A and B peaks are located at 679.62 and 631.80 nm, respectively.²⁵ The XRD data of the MoS₂ sample in Figure 2c shows four peaks at $2\theta \approx 14.4^\circ$, 29.08° , 33.08° , and 44.4° which correspond to (002), (004), (101), and (006) of MoS₂ (JCPDS Card No. 37–1492). The high intensity and sharp peaks of MoS₂ in XRD pattern revealed high purity of the synthesized MoS₂ flakes and confirm that the film does not contain any impurity. Figure 2d shows a schematic of the fabricated gas sensing device on mixed MoS₂

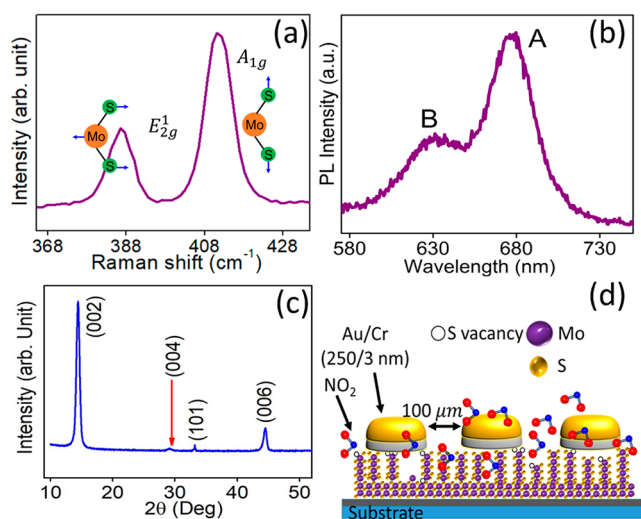


Figure 2. (a) Raman spectra obtained from the mixed MoS₂ flakes. (b) PL spectra were taken at the same area as the Raman measurements. (c) XRD spectra showed the uniformity and purity of the MoS₂ flakes. (d) 3D schematic NO₂ gas sensor from mixed MoS₂ flakes.

structures. Mixed MoS₂ flakes are electrically connected with each other. Gas molecules interacted with the exposed area and changed the resistance of the mixed MoS₂ flake film. *I*–*V* characteristic for the NO₂ sensing at RT and 125 °C with 10 ppm concentration is shown in Supporting Information Figure S2a,b.

We performed NO₂ gas sensing measurements for the four different concentrations of NO₂ (10, 50, 100, and 500 ppm) at the two temperatures RT and 125 °C, respectively. We also performed NO₂ sensing measurements at lower temperatures of 75 and 100 °C. It has been observed that the sensor has no recovery at the lower temperature. However, it shows the full recovery starting at 125 °C. Thus, for the optimum performance of the sensor, we have chosen 125 °C as sensing temperature. Figure 3a,b shows sensor performance in terms of resistance vs time profile for the NO₂ gas at RT and 125 °C, respectively. The response time of mixed MoS₂ flakes at RT and 125 °C for NO₂ gas is presented in Figure 3c,d, respectively. At RT, our device shows the lowest response time of 8.51 s for 10 ppm of NO₂ concentration. Response time is increased with an increase in NO₂ gas concentration and ranged from 8.51 to 26.87 s. However, no recovery happened with the mixed MoS₂ flake sensor at RT. In the case of 125 °C, response time decreased in comparison to the response time at RT, and for all four concentrations it ranges from 4.44 to 8.14 s. Figure 3e shows the recovery time profile for 125 °C. The lowest recovery time observed at 125 °C for 10 ppm is 19.60 s while with 500 ppm it is observed to be around 495.30 s. Figure 3f shows the comparative sensitive profile with different NO₂ concentrations at RT and 125 °C. Sensitivity ($(R_{\text{gas}} - R_{\text{air}})/R_{\text{air}}$) at RT is observed higher than 125 °C. For 10 ppm NO₂ concentration, sensitivity at RT and 125 °C is –10.36% and –7.79%, respectively. The negative change in sensitivity corresponds to decrease in the resistance due to NO₂ exposure. From the results above, it is clear that as NO₂ gas is exposed to mixed MoS₂ flakes the resistance of the sensor decreases. Since NO₂ has the electron acceptor nature and withdraws the electron from the MoS₂ flakes, the decrease in the resistance of mixed MoS₂ flake-based sensor with NO₂ exposure clearly shows its p-type nature.

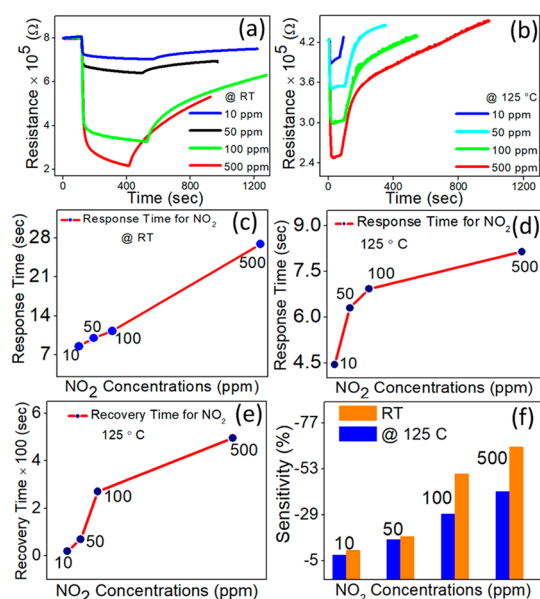


Figure 3. Resistance vs time profile for NO₂ gas sensing at (a) RT and (b) 125 °C for 10, 50, 100, and 500 ppm of NO₂ gas. Corresponding response time curve with the NO₂ exposure at (c) RT and (d) 125 °C. (e) Recovery time profile at 125 °C. Recovery is not observed at room temperature due to high adsorption energy of NO₂ molecules with the MoS₂ flakes. (f) Comparative sensitivity profile for RT and 125 °C. Sensitivity at RT is much higher than at 125 °C due to the easy absorbance of the NO₂ molecules with MoS₂ flakes.

There are several reasons reported for the p-type behavior of MoS₂ flakes like substrate induced charge, charge transfer between the metal and the MoS₂, functionalizing the MoS₂ surface with the metals, defects arise during the CVD synthesis, plasma treatment, and controlled doping of the p-type dopants like oxygen adsorption on MoS₂ flakes.^{26–28} Recently, Neal et al. reported that the incorporated oxygen acts as the p-type dopants for the MoS₂. In our study, the oxygen adsorbed on the MoS₂ flakes or interaction of in-plane MoS₂ with SiO₂/Si substrate may induce controlled p-type doping in mixed MoS₂ flakes.

It can be seen from Figure 3a,b that as the NO₂ gas concentration increases sensor resistance decreases. With the higher concentration of NO₂, as more molecules interacted with the mixed MoS₂ flakes and withdrew more electrons from the surface, it resulted in further change in sensor resistance. The response time at RT in Figure 3c increased with an increase in NO₂ concentration which is due to the interaction of a higher concentration of NO₂ gas molecules with mixed MoS₂ flakes. In the case of 125 °C, the device takes less time to respond to NO₂ gas for each concentration in comparison to RT because the heating of the device may generate new electron–hole pairs, and NO₂ gas molecules quickly adsorb these electrons and thus increase the hole concentration in MoS₂. Hence, the device responds quickly to the NO₂ molecules. The recovery only happened at moderate temperature and not for the RT as the adsorption energy of the NO₂ gas molecule with the MoS₂ flakes is very high at RT.²⁹ However, the heating of the device reduced the adsorption rate of gas molecules with sensor materials and reduced the sensitivity of the sensor.^{30,31} The selectivity of the mixed MoS₂ flake sensor is performed for five different gases, H₂S, H₂, NH₃, and CO₂ with 500 ppm concentration at 125 °C and the results

are shown in Figure 4. The resistance vs time profile is plotted in Figure 4a. The highest change in the resistance takes place

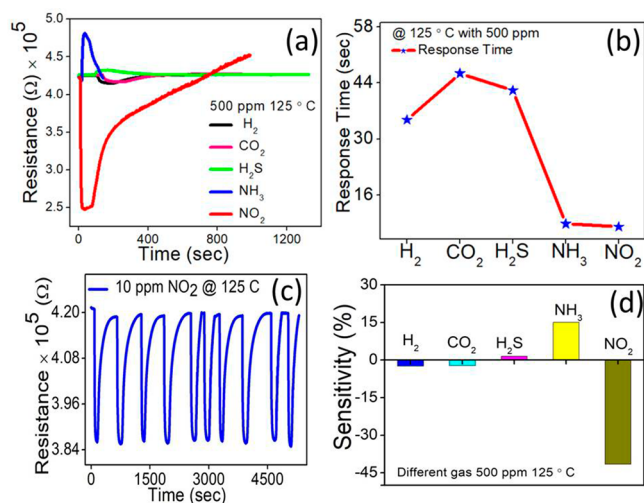


Figure 4. (a) Resistance vs time profile with different gases at 125 °C with 500 ppm concentration of each gas. (b) Response time profile for different gases. (c) Cyclability test for 10 ppm of NO_2 at 125 °C. (d) Selectivity measurements for the gas sensing device.

for the NO_2 gas. The response time and recovery time are plotted in Figure 4b. The response time for the NO_2 was found to be 8.14 s which is again the lowest for NO_2 gas. Reproducibility of the device is calculated for the 10 cycles at 10 ppm NO_2 concentration at 125 °C. The cyclability data clearly showed that sensing is not affected with the span of time. Sensitivity is nearly the same for all the cycles. The selectivity profile, in Figure 4d, revealed that the device has specific sensitivity for the different gases and possess the highest selectivity for the NO_2 gas. Figure 4a shows resistance increases for electron donor gases (H_2S and NH_3) and decreases with the electron acceptor gases (H_2 , CO_2 , and NO_2) which further confirm the p-type nature of our sensing device. Under identical conditions for all the gases, resistance changes largely for the NO_2 gas as shown in Figure 4a, which implies that the mixed MoS_2 flakes provide the most favorable adsorption sites for the NO_2 gas molecules. As in our previous study of the hydrogen gas sensing, we fabricated the hydrogen gas sensing device based on highly uniform edge-enriched MoS_2 flakes which shows the lowest response time and sensitivity of around 14.33 s and 11%, respectively. However, in the present study, the device possesses the mixed flakes of in-plane and edge-enriched MoS_2 flakes.^{11,29} Thus, the response time for hydrogen gas is higher than that of the reported hydrogen sensor due to lower availability of the favorable adsorption sites, edges of the MoS_2 flakes, for the hydrogen molecules. Correspondingly, sensitivity decreased up to 2.38% at 125 °C.¹¹

For CO_2 and H_2S gases, the response time was 46.37 and 42.14 s. The response time is lowest for the NO_2 gas which clearly revealed the highly sensitive nature of the sensor for the NO_2 gas in the presence of the other gases. Also, the sensitivity is highest for the NO_2 gas in comparison to other gases which confirms the highly selective nature of the mixed MoS_2 flakes.

The above results clearly show the good performance of mixed MoS_2 flakes for NO_2 gas at room temperature; however, no recovery was observed. Also, the sensitivity of the sensor reduced from -10.36% to -7.79% at moderate temperature to

achieve the recovery of the sensor. Therefore, to achieve the recovery even at RT, we illuminated the sensor with the UV light during the duration of the entire experiment. The sensor was tested at RT with NO_2 gas in the presence of 365 nm UV light for 10 ppm of NO_2 gas.

The sensitivity profile for four cycles of the 10 ppm NO_2 concentration at RT with UV light illumination is shown in Figure 5a. The UV light illumination not only increased the

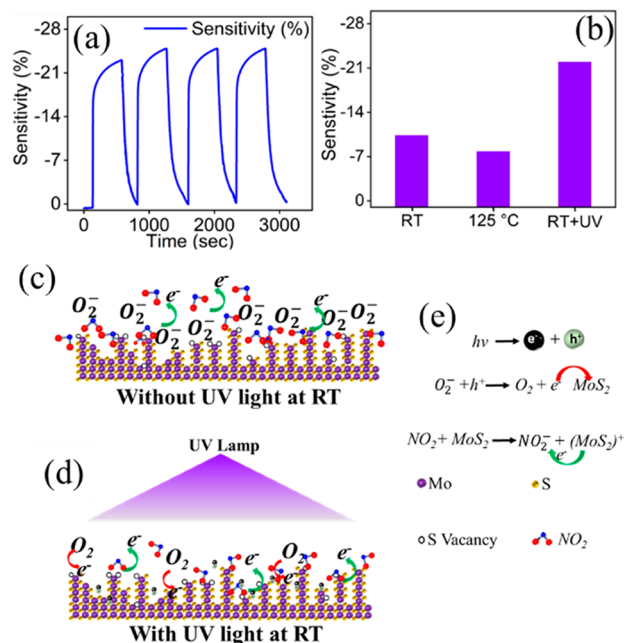


Figure 5. (a) Cyclic profile for the NO_2 gas at RT with UV light illumination. (b) Sensitivity performance of the mixed MoS_2 flakes based gas sensor for the NO_2 gas concentration of 10 ppm. Under UV light illumination sensitivity is increased in comparison to RT and 125 °C. (c) Schematic illustration of the interaction of the NO_2 molecules at RT with the mixed MoS_2 flakes, and (d) at RT with UV light illumination. (e) Possible reactions on the surface of the mixed MoS_2 flakes with NO_2 interaction in the presence of UV light.

sensitivity of the sensor from -10.36% to -21.78% but also decreased the response time from 8.51 to 6.09 s for 10 ppm of the NO_2 sensor in contrast to RT sensor performance. The sensor is observed to have full recovery. The comparison of sensitivity for 10 ppm of NO_2 concentration at RT, 125 °C, and RT with UV light is shown in Figure 5b. UV light illumination clearly increases the sensitivity of the sensor for NO_2 gas. The response time, recovery time, and sensitivity for the RT, 125 °C, and UV light illumination at RT are tabulated in Table 1. To explain the UV assisted enhancement in sensitivity and recovery, we proposed the photoactivated desorption of adsorbed oxygen and creation of fresh active sites on the edges of MoS_2 flakes. In the case of MoS_2 , the edges possess highly active sites in the form of the S vacancy.^{11,20,22} The oxygen adsorbed on the S vacancy and formed O_2^- ions as shown in Figure 5c at RT. UV light illumination triggered the generation of the photoexcited carriers (electron and hole pairs) in mixed MoS_2 flakes.³² The adsorbed oxygen takes the holes from the mixed MoS_2 film and desorbed from the mixed MoS_2 flakes. The desorbed oxygen created new active sites on MoS_2 flakes for the NO_2 molecule adsorption. In the case of heating, the mixed MoS_2 flakes also desorbed O_2^- ions and make the newly fresh adsorption sites available.^{22,33,34} However,

Table 1. Reported Literature of NO₂ Based Gas Sensing on Bare MoS₂ and Hybrid MoS₂ Structures in Comparison with the Present Work on Mixed MoS₂ Flake Structures

sample no	sensing material	S (%)	conc. (ppm)	T (°C)	res time (s)	rec time (s)	ref.
1.	Monolayer MoS ₂	6.1	1.2	RT	>1800	>1800	14
2.	MoS ₂ – Pt NPs	16	1.2	RT	-	-	14
3.	Thin layered MoS ₂	54	100	RT	180	600	36
4.	MoS ₂ /SnO ₂	0.6	0.5	RT	78	84	37
5.	MoS ₂ -Graphene Fiber	62	100	RT	-	-	16
6.	MoS ₂ flakes	10	100	RT	-	-	12
7.	3D-MoS ₂ sphere	78	50	150	-	-	38
8.	In-plane MoS ₂	27.92	100	RT	249	-	35
9.	In-plane MoS ₂	21.56	100	100	71	310	35
10.	In-plane MoS ₂	35.16	100	RT+UV	29	350	35
11.	Graphene/MoS ₂	3	1.2	150	300	672	15
12.	MoS ₂ /Graphene	8	0.5	200	<60	<60	17
13.	Mixed MoS ₂ flakes	-10.36	10	RT	8.51	-	Present Work
14.	Mixed MoS ₂ flakes	-7.79	10	125	4.44	19.6	Present Work
15.	Mixed MoS ₂ flakes	-21.78	10	RT+UV	6.09	146.49	Present Work

Table 2. Calculated adsorption energies and charge transfer for the gases at different sites of MoS₂ flakes

Gas	H Site		T _M Site		T _S Site		B Site	
	E _a (meV)	ΔQ (e)						
NO ₂	-276	0.1	-	-	-249	0.119	-249	0.114
NH ₃	-250	-0.069	-222	-0.051	-100	-0.024	-	-
H ₂	-70	0.004	-82	0.004	-49	0.008	-	-

due to heating, desorption of NO₂ molecules is higher than the adsorption of the NO₂. Hence, the recovery time at 125 °C is much lower than the recovery with UV light at RT. Also, UV light illumination desorbed the O₂⁻ ions more efficiently in comparison to the heating of the device.^{34,35} This is observed from the base resistance of the device without the NO₂ exposure. The base resistance at RT, 125 °C, and with UV illumination at RT was 0.80 MΩ, 0.42 MΩ, and 0.39 MΩ, respectively. The base resistance is lowest for the device illuminated with the UV light, which clearly revealed greater removal of the adsorbed O₂⁻ ions due to the UV light. The schematic of NO₂ adsorption in the presence of the UV light is shown in Figure 5d. The availability of fresher sites increases NO₂ gas molecule adsorption, and thus the sensitivity is increased in the presence of the UV light at RT. The possible reactions at the surface of the mixed MoS₂ structures with NO₂ exposure and by the UV light illumination is shown in the Figure 5e. Table 1 presents the detailed comparison of our NO₂ gas sensing results of mixed MoS₂ flakes with MoS₂ and hybrid MoS₂ nanostructures, reported in the literature.

It is important to note that very large or no recovery time is reported for NO₂ gas with MoS₂ flakes or MoS₂ based composite.^{14,15,29} In our case, the response time of 8.51 s at RT is the lowest response time reported with the mixed structures of MoS₂ flakes, while at the moderate temperature (125 °C) the response time further decreases to 4.44 s. At high temperature we observed the fast recovery of NO₂ gas with the recovery time of 19.60 s. The more detailed comparison of different sensors with the present work is summarized and reported in Table S1 of the Supporting Information. It can be seen clearly from the literature that the traditional metal oxide may have higher sensitivity but needs to be operated at the higher temperature with long response and recovery times. However, the mixed MoS₂ based sensor clearly shows that the sensor is very fast and recoverable with good sensitivity even at

RT and moderate temperature due to its large surface to volume ratio, fast charge transport across the edges, and availability of the favorable adsorption sites in comparison to the other traditional oxide sensors. Moreover, mixed MoS₂ flake sensors working under UV illumination show completely reversible, fast, and highly sensitive NO₂ gas sensor than bare and hybrid MoS₂ nanostructures reported in the literature.

To understand our experimental finding, we considered the density functional theory (DFT) calculation. The interaction of the gas molecules completely depends on the adsorption energy on the surface. The adsorption energy is given by $E_a = E_{\text{MoS}_2 + \text{molecule}} - (E_{\text{MoS}_2} + E_{\text{gas molecule}})$ where $E_{\text{MoS}_2 + \text{molecule}}$ is the total energy of the adsorbed gas molecule on MoS₂, E_{MoS_2} is the energy of the MoS₂ layer, and $E_{\text{gas molecule}}$ is the energy of the separate gas molecule.³⁹ Another important parameter is the charge transfer between the gas molecule and the MoS₂ flakes. Charge transfer is positive if charge transfer from the MoS₂ to the gas molecule and gas is said to be a charge acceptor, or if the charge transfer is from the gas molecule to MoS₂, then the gas is said to be a charge donor.^{39,40} It is reported that the adsorption of the target gas molecules is favorable for some particular MoS₂ sites.³⁹ Yue and co-workers studied the adsorption of the NO₂, NH₃, and H₂ gas molecules on the MoS₂ at four available sites, H site (top of the MoS₂ hexagon), T_M site (top of Mo atoms), T_S site (top of S atoms), and B site (top of Mo–S bonds).³⁹ The calculated adsorption energy for the NO₂, NH₃, and H₂ molecules is summarized in Table 2. The highest negative adsorption energy is for the NO₂ molecules for all the sites, except the T_M site, as no data is reported. In our case, we have mixed MoS₂ flakes which provide enough favorable adsorption sites for the NO₂ at the H, T_S, and B sites. So, the mixed MoS₂ is highly sensitive for NO₂ gas adsorption. For NH₃ adsorption, the favorable sites are at the H, T_M, and T_S sites, but the adsorption energy is less for the T_M and T_S sites. So, the mixed MoS₂ flakes are highly favorable for

the NO_2 in comparison to NH_3 . Due to the very high adsorption energy of NO_2 gas molecules at the sites mentioned, the recovery does not happen at the RT from mixed MoS_2 flakes. In the case of the H_2 molecule, the higher adsorption energy is available at the T_M , T_S , and B sites. So, hydrogen adsorption is not very fast due to lack of T_M and T_S in mixed MoS_2 structure.^{11,39} This behavior of hydrogen agrees well with our previous study.¹¹

For CO_2 and NH_3 gases, the adsorption behavior and charge transfer on pristine MoS_2 and MoS_2 possessing sulfur vacancies (defective MoS_2) were investigated.⁴¹ It was observed that the adsorption and charge transfer with the defective MoS_2 had higher values in comparison to that of pristine MoS_2 . In the case of CO_2 , the most favorable site is the B site where the presence of S vacancies makes the adsorption higher with the adsorption energy of 171 meV in contrast to 139 meV for pristine MoS_2 . The positive charge transfer of 0.0279e validates the electron accepting behavior which is also confirmed by the sensitivity profile for CO_2 with our sensing device. With NH_3 gas, the adsorption energy is 0.407 eV with the negative charge transfer of the $-0.0615e$ which revealed its electron donor nature above the Mo–S bond.⁴¹ There is no detailed DFT calculation study reported for the H_2S gas in the literature. Figure 6a shows the graph between the charge transfer and the

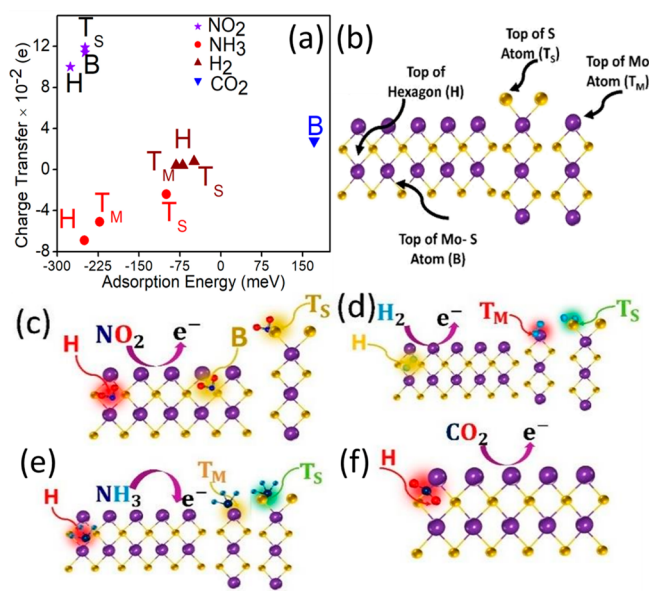


Figure 6. (a) Charge transfer vs adsorption energy profile for NO_2 , NH_3 , H_2 , and CO_2 gases. (b) Possible favorable adsorption sites available with MoS_2 . (c–f) Adsorption of gases on the favorable sites. The red colored region shows the highest adsorption site, the yellow region site shows the the lower adsorption site, and the green region shows the lowest adsorption sites. NO_2 , H_2 , and CO_2 behave as electron acceptors while NH_3 behaves as an electron donor.

adsorption energy and Figure 6b shows the adsorption sites with the different gases. From the above discussion, it is clear that our mixed structure based MoS_2 device has very high sensitivity for the NO_2 gas in comparison to the other gases NH_3 , H_2 , CO_2 , and H_2S . The presence of favorable sites in the mixed MoS_2 flakes makes the device more reliable for sensing of the target gas.

The very high adsorption energy of the NO_2 gas at the H-site the T_M site, and the B site makes the device faster, more

sensitive, and more selective for the NO_2 gas molecules even at RT.

CONCLUSION

In conclusion, we synthesized p-type mixed MoS_2 flakes on the SiO_2/Si substrate in a modified chemical vapor deposition system and demonstrated a photoactivated NO_2 sensor at room temperature. The mixed MoS_2 based sensor shows complete recovery and fast response in photoactive and thermally active mode at room temperature and at 125 °C, respectively. The sensor was observed to be highly selective for NO_2 sensing against H_2 , H_2S , CO_2 , and NH_3 gases. The adsorption of target gas on favorable sites of MoS_2 flakes was discussed as one of the main reasons for highly selective, sensitive, and fast response of mixed MoS_2 flake-based gas sensor.

ASSOCIATED CONTENT

Supporting Information

The Supporting Information is available free of charge on the ACS Publications website at DOI: 10.1021/acssensors.8b00146.

Schematic of modified atmospheric CVD setup and growth temperature profile. I – V characteristics with and without NO_2 exposure at RT and 125 °C. Resistance vs time profile at RT with UV light. Table for different NO_2 sensors and comparison with present work (PDF)

AUTHOR INFORMATION

Corresponding Author

*E-mail: mkumar@iitrpr.ac.in.

ORCID

Abhay. V. Agrawal: 0000-0002-2940-6050

Alex Zakhidov: 0000-0001-6980-2659

Mahesh Kumar: 0000-0002-5357-7300

Mukesh Kumar: 0000-0001-6389-2040

Author Contributions

A.V.A. wrote the manuscript, grew MoS_2 samples, and analyzed all of the data presented in this manuscript under the supervision of Mukesh Kumar; R.K. and Mahesh Kumar performed gas sensing measurement. S.V. and A.Z. performed FE-SEM, EDS, and XRD measurement. G.Y. and J.B. did Raman and PL measurement. All authors participated in the discussion and interpretation of the results and commented on the manuscript.

Notes

The authors declare no competing financial interest.

ACKNOWLEDGMENTS

The authors acknowledge the Department of Atomic Energy (DAE) under Project No. 34/20/09/2015/BRNS and also the Department of Physics, IIT Ropar for providing financial support and the research facility.

REFERENCES

- (1) Hadley, M. B.; Vedanthan, R.; Fuster, V. Air pollution and cardiovascular disease: a window of opportunity. *Nat. Rev. Cardiol.* **2018**, *15*, 193.
- (2) Yamazoe, N. Toward innovations of gas sensor technology. *Sens. Actuators, B* **2005**, *108* (1), 2–14.
- (3) Victor, D. G.; Ramanathan, V.; Zaelke, D. Harmful soot spurs climate-policy action. *Nature* **2015**, *517*, 21.

- (4) Reis, S.; Grennfelt, P.; Klimont, Z.; Amann, M.; ApSimon, H.; Hettelingh, J.-P.; Holland, M.; LeGall, A.-C.; Maas, R.; Posch, M.; Spranger, T.; Sutton, M. A.; Williams, M. From Acid Rain to Climate Change. *Science* **2012**, *338* (6111), 1153–1154.
- (5) Vanalakar, S. A.; Patil, V. L.; Harale, N. S.; Vhanalakar, S. A.; Gang, M. G.; Kim, J. Y.; Patil, P. S.; Kim, J. H. Controlled growth of ZnO nanorod arrays via wet chemical route for NO₂ gas sensor applications. *Sens. Actuators, B* **2015**, *221*, 1195–1201.
- (6) Mane, A. A.; Moholkar, A. V. Effect of film thickness on NO₂ gas sensing properties of sprayed orthorhombic nanocrystalline V₂O₅ thin films. *Appl. Surf. Sci.* **2017**, *416*, 511–520.
- (7) Chougule, M. A.; Sen, S.; Patil, V. B. Fabrication of nanostructured ZnO thin film sensor for NO₂ monitoring. *Ceram. Int.* **2012**, *38* (4), 2685–2692.
- (8) Splendiani, A.; Sun, L.; Zhang, Y.; Li, T.; Kim, J.; Chim, C. Y.; Galli, G.; Wang, F. Emerging Photoluminescence in Monolayer MoS₂. *Nano Lett.* **2010**, *10*, 1271–1275.
- (9) Bollinger, M. V.; Lauritsen, J. V.; Jacobsen, K. W.; Nørskov, J. K.; Helveg, S.; Besenbacher, F. One-Dimensional Metallic Edge States in MoS₂. *Phys. Rev. Lett.* **2001**, *87* (19), 196803.
- (10) Jaramillo, T. F.; Jørgensen, K. P.; Bonde, J.; Nielsen, J. H.; Horch, S.; Chorkendorff, I. Identification of Active Edge Sites for Electrochemical H₂ Evolution from MoS₂ Nanocatalysts. *Science* **2007**, *317* (5834), 100–102.
- (11) Agrawal, A. V.; Kumar, R.; Venkatesan, S.; Zakhidov, A.; Zhu, Z.; Bao, J.; Kumar, M.; Kumar, M. Fast detection and low power hydrogen sensor using edge-oriented vertically aligned 3-D network of MoS₂ flakes at room temperature. *Appl. Phys. Lett.* **2017**, *111* (9), 093102.
- (12) Cho, S.-Y.; Kim, S. J.; Lee, Y.; Kim, J.-S.; Jung, W.-B.; Yoo, H.-W.; Kim, J.; Jung, H.-T. Highly Enhanced Gas Adsorption Properties in Vertically Aligned MoS₂ Layers. *ACS Nano* **2015**, *9* (9), 9314–9321.
- (13) Liu, B.; Chen, L.; Liu, G.; Abbas, A. N.; Fathi, M.; Zhou, C. High-Performance Chemical Sensing Using Schottky-Contacted Chemical Vapor Deposition Grown Monolayer MoS₂ Transistors. *ACS Nano* **2014**, *8* (5), 5304–5314.
- (14) He, Q.; Zeng, Z.; Yin, Z.; Li, H.; Wu, S.; Huang, X.; Zhang, H. Fabrication of Flexible MoS₂ Thin-Film Transistor Arrays for Practical Gas-Sensing Applications. *Small* **2012**, *8* (19), 2994–2999.
- (15) Cho, B.; Yoon, J.; Lim, S. K.; Kim, A. R.; Kim, D.-H.; Park, S.-G.; Kwon, J.-D.; Lee, Y.-J.; Lee, K.-H.; Lee, B. H.; Ko, H. C.; Hahm, M. G. Chemical Sensing of 2D Graphene/MoS₂ Heterostructure device. *ACS Appl. Mater. Interfaces* **2015**, *7* (30), 16775–16780.
- (16) Niu, Y.; Wang, R.; Jiao, W.; Ding, G.; Hao, L.; Yang, F.; He, X. MoS₂ graphene fiber based gas sensing devices. *Carbon* **2015**, *95*, 34–41.
- (17) Long, H.; Harley-Trochimczyk, A.; Pham, T.; Tang, Z.; Shi, T.; Zettl, A.; Carraro, C.; Worsley, M. A.; Maboudian, R. High Surface Area MoS₂/Graphene Hybrid Aerogel for Ultrasensitive NO₂ Detection. *Adv. Funct. Mater.* **2016**, *26* (28), 5158–5165.
- (18) Dey, S.; Matte, H. S. S. R.; Shirodkar, S. N.; Waghmare, U. V.; Rao, C. N. R. Charge-Transfer Interaction between Few-Layer MoS₂ and Tetrathiafulvalene. *Chem. - Asian J.* **2013**, *8* (8), 1780–1784.
- (19) Lukowski, M. A.; Daniel, A. S.; Meng, F.; Forticaux, A.; Li, L.; Jin, S. Enhanced Hydrogen Evolution Catalysis from Chemically Exfoliated Metallic MoS₂ Nanosheets. *J. Am. Chem. Soc.* **2013**, *135* (28), 10274–10277.
- (20) Nan, H.; Wang, Z.; Wang, W.; Liang, Z.; Lu, Y.; Chen, Q.; He, D.; Tan, P.; Miao, F.; Wang, X.; Wang, J.; Ni, Z. Strong Photoluminescence Enhancement of MoS₂ through Defect Engineering and Oxygen Bonding. *ACS Nano* **2014**, *8* (6), 5738–5745.
- (21) Zhang, Y. H.; Chen, Y. B.; Zhou, K. G.; Liu, C. H.; Zeng, J.; Zhang, H. L.; Peng, Y. Improving gas sensing properties of graphene by introducing dopants and defects: a first-principles study. *Nanotechnology* **2009**, *20* (18), 185504.
- (22) Burman, D.; Ghosh, R.; Santra, S.; Kumar Ray, S.; Kumar Guha, P. Role of vacancy sites and UV-ozone treatment on few layered MoS₂ nanoflakes for toxic gas detection. *Nanotechnology* **2017**, *28* (43), 435502.
- (23) Lee, C.; Yan, H.; Brus, L. E.; Heinz, T. F.; Hone, J.; Ryu, S. Anomalous Lattice Vibrations of Single- and Few-Layer MoS₂. *ACS Nano* **2010**, *4* (5), 2695–2700.
- (24) Verble, J. L.; Wieting, T. J. Lattice Mode Degeneracy in MoS₂ and Other Layer Compounds. *Phys. Rev. Lett.* **1970**, *25* (6), 362–365.
- (25) Splendiani, A.; Sun, L.; Zhang, Y.; Li, T.; Kim, J.; Chim, C.-Y.; Galli, G.; Wang, F. Emerging Photoluminescence in Monolayer MoS₂. *Nano Lett.* **2010**, *10* (4), 1271–1275.
- (26) Dolui, K.; Rungger, I.; Sanvito, S. Origin of the n-type and p-type conductivity of MoS₂ monolayers on a SiO₂ substrate. *Phys. Rev. B: Condens. Matter Mater. Phys.* **2013**, *87* (16), 165402.
- (27) Min, S.-W.; Yoon, M.; Yang, S. J.; Ko, K. R.; Im, S. Charge-Transfer-Induced p-Type Channel in MoS₂ Flake Field Effect Transistors. *ACS Appl. Mater. Interfaces* **2018**, *10* (4), 4206–4212.
- (28) Neal, A. T.; Pachter, R.; Mou, S. P-type conduction in two-dimensional MoS₂ via oxygen incorporation. *Appl. Phys. Lett.* **2017**, *110* (19), 193103.
- (29) Cho, B.; Hahm, M. G.; Choi, M.; Yoon, J.; Kim, A. R.; Lee, Y.-J.; Park, S.-G.; Kwon, J.-D.; Kim, C. S.; Song, M.; Jeong, Y.; Nam, K.-S.; Lee, S.; Yoo, T. J.; Kang, C. G.; Lee, B. H.; Ko, H. C.; Ajayan, P. M.; Kim, D.-H. Charge-transfer-based Gas Sensing Using Atomic-layer MoS₂. *Sci. Rep.* **2015**, *5*, 8052.
- (30) Yavari, F.; Chen, Z.; Thomas, A. V.; Ren, W.; Cheng, H.-M.; Koratkar, N. High Sensitivity Gas Detection Using a Macroscopic Three-Dimensional Graphene Foam Network. *Sci. Rep.* **2011**, *1*, 166.
- (31) Choi, H.; Choi, J. S.; Kim, J.-S.; Choe, J.-H.; Chung, K. H.; Shin, J.-W.; Kim, J. T.; Youn, D.-H.; Kim, K.-C.; Lee, J.-L.; Choi, S.-Y.; Kim, P.; Choi, C.-G.; Yu, Y.-J. Flexible and Transparent Gas Molecule Sensor Integrated with Sensing and Heating Graphene Layers. *Small* **2014**, *10* (18), 3685–3691.
- (32) Bao, J.; Shalish, I.; Su, Z.; Gurwitz, R.; Capasso, F.; Wang, X.; Ren, Z. Photoinduced oxygen release and persistent photoconductivity in ZnO nanowires. *Nanoscale Res. Lett.* **2011**, *6* (1), 404.
- (33) Chen, T.-C.; Yang, Y.-C.; Liu, H.-L.; Yang, C.-M.; Meyyappan, M.; Lai, C.-S. The Effect of Monolayer Graphene on the UV Assisted NO₂ Sensing and Recovery at Room Temperature. *Proceedings* **2017**, *1* (4), 461.
- (34) Khan, M. F.; Iqbal, M. W.; Iqbal, M. Z.; Shehzad, M. A.; Seo, Y.; Eom, J. Photocurrent Response of MoS₂ Field-Effect Transistor by Deep Ultraviolet Light in Atmospheric and N₂ Gas Environments. *ACS Appl. Mater. Interfaces* **2014**, *6* (23), 21645–21651.
- (35) Kumar, R.; Goel, N.; Kumar, M. UV-Activated MoS₂ Based Fast and Reversible NO₂ Sensor at Room Temperature. *ACS Sensors* **2017**, *2* (11), 1744–1752.
- (36) Late, D. J.; Huang, Y.-K.; Liu, B.; Acharya, J.; Shirodkar, S. N.; Luo, J.; Yan, A.; Charles, D.; Waghmare, U. V.; Dravid, V. P.; Rao, C. N. R. Sensing Behavior of Atomically Thin-Layered MoS₂ Transistors. *ACS Nano* **2013**, *7* (6), 4879–4891.
- (37) Cui, S.; Wen, Z.; Huang, X.; Chang, J.; Chen, J. Stabilizing MoS₂ Nanosheets through SnO₂ Nanocrystal Decoration for High-Performance Gas Sensing in Air. *Small* **2015**, *11* (19), 2305–2313.
- (38) Yu, L.; Guo, F.; Liu, S.; Qi, J.; Yin, M.; Yang, B.; Liu, Z.; Fan, X. H. Hierarchical 3D flower-like MoS₂ spheres: Post-thermal treatment in vacuum and their NO₂ sensing properties. *Mater. Lett.* **2016**, *183*, 122–126.
- (39) Yue, Q.; Shao, Z.; Chang, S.; Li, J. Adsorption of gas molecules on monolayer MoS₂ and effect of applied electric field. *Nanoscale Res. Lett.* **2013**, *8* (1), 425.
- (40) Ganji, M. D.; Sharifi, N.; Ghorbanzadeh Ahangari, M.; Khosravi, A. Density functional theory calculations of hydrogen molecule adsorption on monolayer molybdenum and tungsten disulfide. *Phys. E* **2014**, *57*, 28–34.
- (41) Li, H.; Huang, M.; Cao, G. Markedly different adsorption behaviors of gas molecules on defective monolayer MoS₂: a first-principles study. *Phys. Chem. Chem. Phys.* **2016**, *18* (22), 15110–15117.